

1-24-1987

## Correlative Light and Electron Microscopy of Platelet Adhesion and Fibrinogen Receptor Expression using Colloidal-Gold Labeling

Steven L. Goodman  
*University of Wisconsin*

Ralph M. Albrecht  
*University of Wisconsin*

Follow this and additional works at: <https://digitalcommons.usu.edu/microscopy>



Part of the [Life Sciences Commons](#)

---

### Recommended Citation

Goodman, Steven L. and Albrecht, Ralph M. (1987) "Correlative Light and Electron Microscopy of Platelet Adhesion and Fibrinogen Receptor Expression using Colloidal-Gold Labeling," *Scanning Microscopy*. Vol. 1 : No. 2 , Article 29.

Available at: <https://digitalcommons.usu.edu/microscopy/vol1/iss2/29>

This Article is brought to you for free and open access by the Western Dairy Center at DigitalCommons@USU. It has been accepted for inclusion in Scanning Microscopy by an authorized administrator of DigitalCommons@USU. For more information, please contact [digitalcommons@usu.edu](mailto:digitalcommons@usu.edu).



CORRELATIVE LIGHT AND ELECTRON MICROSCOPY OF PLATELET ADHESION AND FIBRINOGEN  
RECEPTOR EXPRESSION USING COLLOIDAL-GOLD LABELING

Steven L. Goodman and Ralph M. Albrecht\*

Department of Veterinary Science  
University of Wisconsin, Madison, Wisconsin 53706

(Received for publication October 13, 1986, and in revised form January 24, 1987)

Abstract

Differences in the shape change responses of platelets to various polymers may determine the thrombotic potential of these materials. Substrate-dependent variation in the expression and motility of the platelet fibrinogen receptor may underlie these differences due to this ligand's essential role in platelet aggregation. In this study we examine platelet activation on polyetherurethaneureas (PEUUs) presently being evaluated for vascular prosthetic applications. These polymers are prepared as 50-100nm thin films suitable as substrates for consecutive light microscopy, high voltage electron microscopy (HVEM), and SEM. 18nm colloidal gold coupled to fibrinogen permits visualization of that receptor's motility in living cells by video-enhanced light microscopy. Subsequent HVEM and SEM of identified cells provides correlative ultrastructure and surface morphology. The use of these novel support films coupled with the multiple modes of microscopy and colloidal gold labeled ligands permits in depth study of the molecular biology of cell adhesion to materials with varied, and known, surface properties.

The motility of the platelet fibrinogen receptor was related to the extent of cytoskeletal reorganization, which, in turn, was influenced by polymer surface energetics. Platelets adherent to more hydrophobic PEUUs had greater receptor mobility and receptor redistribution than platelets adherent to more hydrophilic PEUUs. The most extensive receptor motility and redistribution was observed on Formvar, a non-PEUU with low surface-water energy, suggesting that additional surface properties are of importance in determining platelet spreading and fibrinogen receptor motility.

Key Words: Platelet, Adhesion, Fibrinogen, Receptor, Light Microscopy, SEM, High Voltage Electron Microscopy (HVEM), Colloidal Gold, Polymers, Biomaterials.

\*Address for Correspondence:  
Ralph M. Albrecht  
University of Wisconsin, Veterinary Science  
1655 Linden Drive  
Madison, WI 53706 Phone No. (608)263-3952

Introduction

In order to further our understanding of artificial surface induced thrombosis and embolization it is important to characterize the events occurring when platelets contact vascular prosthetic materials. The expression and motility of the platelet fibrinogen (FGN) receptor is also of interest due to this ligand's essential role in platelet aggregation (30,31,33). Platelet adhesion can also be used as a model for cellular adhesion. Extensive cytoskeletal reorganization (23,26) accompanies platelet shape change occurring subsequent to initial adherence. The absence of a nucleus in the platelet simplifies both the microscopic observation of these cell fragments and the interpretation of cellular events.

The cytoskeletal events accompanying the shape change of surface activated platelets have been described (22,23,26). Briefly, platelets progress from a discoid shape to a spherical form, then through a series of pseudopodial shapes eventually culminating in a fully spread thin disk. Concomitant with the final stages of this shape change, three distinct cytoskeletal zones develop, each of which circumferentially surrounds the central granule zone. Proceeding outward from the central granule, these zones have been described as the inner filamentous zone (IFZ), the outer filamentous zone, and the peripheral web (25,26). Of importance to the present investigation, Loftus and Albrecht (24,25), using colloidal gold labeled fibrinogen, reported that fibrinogen binds initially to the platelet surface, including the pseudopods and the cell periphery. As spreading proceeds the fibrinogen receptors move towards the central granule while remaining in the plane of the membrane. This inward migration continues, eventually leading to the final localization of the fibrinogen receptors over the IFZ in fully spread platelets.

Many researchers have reported large differences in the extent of platelet shape change for platelets adherent to various polymers (4,6,10,19,29). Previously, we have reported differences in the extent of cytoskeletal reorganization of in vitro platelets adherent to a family of polyetherurethaneureas (PEUUs) (7,8) being examined for their potential for vascular prosthetic

applications (11). Platelets adherent to many of these polymers do not change shape completely and are apparently inhibited in the final stages of shape change during the development of the platelet IFZ (7,8). Since fibrinogen receptor redistribution is related to cytoskeletal reorganization, and in particular is thought to be dependent on the development of the platelet IFZ (24,25), visualization of fibrinogen receptor motility on these materials is of interest. Considering the essential role of fibrinogen in platelet aggregation, which in turn is necessary for the formation of thrombi, understanding how these polymers influence fibrinogen receptor motility may lead to an understanding of how platelet aggregation on polymers leads to thrombosis (10,19).

Since platelet shape change occurs in minutes, observation of living cells by light microscopy is desirable, if not essential, to understand the nuances of adhesion, shape change, and receptor motility. However, to follow receptor expression and motility by light microscopy requires an appropriately labeled ligand. Ideally, this label also should be detectable in electron microscopes so that the previous history of cells being examined for ultrastructure, by electron microscopy, is known. Colloidal gold has been used successfully as an SEM and TEM label for studies of cell surface receptors (1,14,24,25). However, only recently, with the advent of video-enhanced light microscopy (VLM) (2,15), have colloidal gold particles in sizes appropriate for SEM or TEM been detectable by light microscopy.

Our interest is to follow platelet adhesion, shape change, and receptor expression, by VLM and then study the same cells seen by VLM using HVEM and SEM respectively, for their cytoskeletal structure and for their surface morphology. In particular, we wish to characterize differences in cell behavior by all three microscopic modes for platelets adherent to a family of PEUUs with varied surface properties. In order to perform this study we therefore needed to prepare these polymers as substrates suitable for consecutive VLM, HVEM, and SEM. Herein we describe a method for the preparation of these polymers as thin films with acceptable properties for transmitted light and electron microscopy. And, in particular, in this report we demonstrate the feasibility of correlative VLM, HVEM, and SEM of platelet shape change and (colloidal gold labeled) fibrinogen receptor motility, for platelets adherent to PEUUs of biomedical significance and to Formvar.

### Experimental

#### Materials

Six materials were studied for their effects on FGN receptor redistribution. These were Formvar (Monsanto, St. Louis, MO, USA), solution grade Biomer (Ethicon Inc., Somerville, N.J., USA, lot #BSQXXI2), and four laboratory synthesized polyetherurethaneureas (PEUUs).

The four laboratory synthesized PEUUs have been described in detail elsewhere (11). These polymers were prepared in a two-step condensation

reaction in N,N-dimethylacetamide (DMAC, Aldrich Chemicals, Milwaukee, WI, USA). Step one was the reaction between two moles of methylene diphenylene diisocyanate (MDI) with one mole of, one of four, polyols; poly(tetramethylene oxide), hydroxybutyl terminated poly(dimethylsiloxane), poly(propylene oxide), or poly(ethylene oxide) (PTMO, PDMS, PPO, or PEO respectively). All polyols are of 1000 MW except PDMS which has a molecular weight of 2000. This prepolymer was then chain extended with one mole ethylene diamine (ED) in step 2, to form the PEUU. In the subsequent discussion these polymers are referred to by their polyol abbreviation, thus PEO-PEUU is the poly(ethylene oxide) based polyetherurethane-urea.

All five PEUUs; four laboratory synthesized plus solution Biomer (SB), were prepared as 50-100nm thin films by spin-casting from 2-4% solutions in DMAC onto sodium chloride crystal substrates: One cm NaCl cubic crystals (Ted Pella Inc., Tustin, CA, USA) were cleaved in half with single edged razor blades. The resultant pieces were then cleaved in half repeatedly until crystals 1 cm square by 1-2 mm thick remained. These were kept absolutely dry until coated. To spin-cast, a thin NaCl crystal wafer was placed in a 2 mm deep well (1.45cm diameter) in the center of a turntable. Polymer solution was applied to just cover the wafer (2-4 drops) and allowed to remain for 2 minutes. The turntable was then brought to 3000-4000 rpm and maintained at speed for 20 sec while an additional 2 drops of solution were applied. This coating sequence was repeated twice, the crystal wafer was removed, and was then placed on desiccant in a loosely covered petri dish in a fume hood to allow solvent to evaporate in conditions of zero humidity. After 36 h the coated face of the crystal wafer was lightly scored with a scalpel into 2.5 mm grid size squares. The coated and scored crystals were then floated on distilled water. When the films released from the crystal, bare NiCr maxtaform finder grids were inserted below the water surface to pick up the floating films from underneath. Thus the air-cast face of the PEUU films were on top and used as the cell adhesion substrate. The distinction of sidedness is important since polymers orient at interfaces to minimize interfacial energy (32) thereby altering their surface properties (17). The air-cast face of these materials is the surface exposed to blood in virtually all applications.

Formvar filmed grids were prepared by standard methods. Briefly, this consisted of dip-coating microscope slides in 0.35% Formvar in ethylene dichloride, floating the dried Formvar film onto a distilled water surface, and then placing maxtaform finder grids on the floating film. In these studies the glass-cast face of the film was used as the platelet adhesion substrate since most microscopists appear to use some variation of the method described by Hall (12) to prepare filmed grids, and to be consistent with other cell adhesion studies (22-26).

All 5 PEUU materials have been previously analyzed for various surface and bulk properties

(11,20). A summary of their surface energetic properties, obtained by underwater contact angle measurements with air and octane probe fluids (3,13,21), appears in Table 1. The values for the PEUU materials were obtained for several micron thick films, thus caution should be exercised in applying these numbers to the 50-100nm films used in the present study. Briefly, these measured (contact angle) and calculated ( $\gamma_{sw}$  and  $\gamma_{s^p}/\gamma_{s^d}$ ) parameters provide measures of surface hydrophobicity and surface polarity. For example, small contact angle, low  $\gamma_{sw}$ , and high  $\gamma_{s^p}/\gamma_{s^d}$  ratios indicate a relatively hydrophilic and polar surface.

#### Colloidal gold labels

Colloidal gold was prepared by previously described methods (1,9,14,24). 18nm colloidal gold particles were prepared by the reduction of 4% HAuCl<sub>4</sub> (0.5ml) in 200 ml boiling deionized distilled water by the addition of 1% trisodium citrate (5 ml). This mixture was refluxed for 30 min. The formation of the monodisperse colloid caused a color change from dark blue to red. For 24 and 50nm colloidal gold, 3 ml and 1.6 ml of 1% trisodium citrate, respectively, were used as the reductant (9,14).

Fibrinogen (FGN) was purified from citrated human plasma by precipitation with 25% saturated ammonium sulfate followed by DEAE-Cellulose chromatography and dialysis against 0.01 M Tris, 0.14 M NaCl buffer, pH 7.4 (28). FGN was complexed to colloidal gold at pH 6.5, slightly above the pI of FGN, by pH adjustment with 0.2 N K<sub>2</sub>CO<sub>3</sub>. The minimal amount of FGN necessary to stabilize the colloidal gold was determined by adsorption isotherms (9,14,24). Further stabilization was achieved with the addition of a 1% solution of 20,000 MW poly(ethylene glycol). The gold labeled FGN (FGN-Au) was sedimented at 11,000x g for 30 min, resuspended in BSA and dextrose-free Tyrode's buffer (see below) and filtered through a 0.2  $\mu$ m filter. The specificity of these FGN-Au labels for the FGN receptor has been determined (24,25).

#### Platelets

Platelets were purified in a two step process (6,10,24-26). Whole blood was anti-coagulated with 10 mM EGTA and centrifuged at 165x g for 15 min. The resultant platelet-rich-plasma supernatant was then chromatographed on Sepharose 4B (Sigma Chemical, St. Louis, MO, USA) previously equilibrated with calcium-free modified Tyrode's Buffer (136mM NaCl, 2.7mM KCl, 0.42mM NaH<sub>2</sub>PO<sub>4</sub>, 12mM NaHCO<sub>3</sub>, 1mM MgCl<sub>2</sub>, 1g/l dextrose, 2 g/l albumin). This same buffer was also used as the elutriant. Platelets eluted in the void volume.

#### Procedure

The platelet suspensions were supplemented with calcium containing modified Tyrode's (1mM final concentration) immediately prior to pipetting onto the test materials. Polymer filmed grids, one PEUU and one Formvar, were affixed in an open ended chamber constructed of cover glasses, Parafilm (American Can Co., Greenwich, CT, USA), and VALAP (a 1:1:1 mixture of Vaseline, lanolin, and paraffin). This disposable chamber allowed media to be exchanged or supplemented, such as the addition of FGN-Au, while cells were

under continual VLM observation. FGN-Au was added after a sufficient number of platelets had attached to the filmed grids, but prior to the formation of a complete platelet monolayer. Preparations were fixed after 45 min of activation to assure a large population of maximally activated cells. Previous studies have shown that the maximum percentage of fully spread platelets on polymer surfaces under similar conditions occurs at 30-45 min (6,10). Formvar adherent platelets were observed to insure that the cell population was normally activatable. When full spreading and complete colloidal gold labeled fibrinogen (FGN-Au) centralization (24,25) was not observed on the Formvar grid the experiment was discarded.

#### Electron Microscopy

Platelets adherent to grids were fixed in 0.1 M HEPES buffered 1% glutaraldehyde supplemented with 0.5% saponin, 0.2% tannic acid, pH 7.2 for 30 min. Fixative was applied either while the cells were being observed by VLM or immediately upon removal from the microscope stage. After rinsing in the 0.1 M HEPES buffer, platelets were postfixfixed in 0.05% OsO<sub>4</sub> (24,27) in HEPES for 15 min, water rinsed, stained in aqueous uranyl acetate for 15 min, and water rinsed again. Preparations were then dehydrated with graded ethanol to absolute molecular sieve-dried ethanol and dried by the critical point procedure with molecular sieve-dried CO<sub>2</sub> as the transitional fluid.

Grids were stabilized with evaporated carbon applied to the non-cell side and viewed with the Madison, Wisconsin NIH Bioresources AEI High Voltage Electron Microscope (HVEM) at 1000 kV. Stereo-pair micrographs were recorded at magnifications from 5000 to 20,000x for analysis. Following HVEM examination, specimens were sputter coated (triode type instrumentation) with 10-15nm of AuPd prior to secondary electron imaging with a JEOL JSM 35C SEM at 10-15 kV.

#### Light Microscopy

The light microscope used was an inverted Nikon Diaphot (Garden City, NY, USA) modified for increased light transmittance to the TV camera. In this study, condenser (polarization) rectified (16) differential interference contrast (DIC) imaging (2,15) was done with a wavelength of 546nm, using a 1.25 NA 100x plan apochromatic objective. Images were projected to the TV camera giving a final, optical plus electronic,

Material	Contact Angle		Energetics		ref.
	$\theta_{aw}$	$\theta_{ow}$	$\gamma_{sw}$	$\gamma_{s^p}/\gamma_{s^d}$	
MDI/ED/polyol					
PTMO 1000 MW	58±5	98±6	23	0.19	(11)
PDMS 2000 MW	108±5	132±7	36	0.11	(11)
PPO 1000 MW	60±2	89±4	14	0.35	(11)
PEO 1000 MW	51±5	71±5	6.3	0.76	(11)
Solution Biomer	56	76	7.7	0.66	(20)
Formvar	38±4	54±4	2.4	1.19	

Table 1. Materials and surface properties. Materials are as described in Methods. Air-water ( $\theta_{aw}$ ) and octane-water ( $\theta_{ow}$ ) contact angles in degrees appear as mean±SD. Surface-water interfacial energy ( $\gamma_{sw}$ ) is in dynes/cm, and the ratio of the polar and dispersive components of the solid surface energy ( $\gamma_{s^p}/\gamma_{s^d}$ ) were approximated with the geometric mean equation.

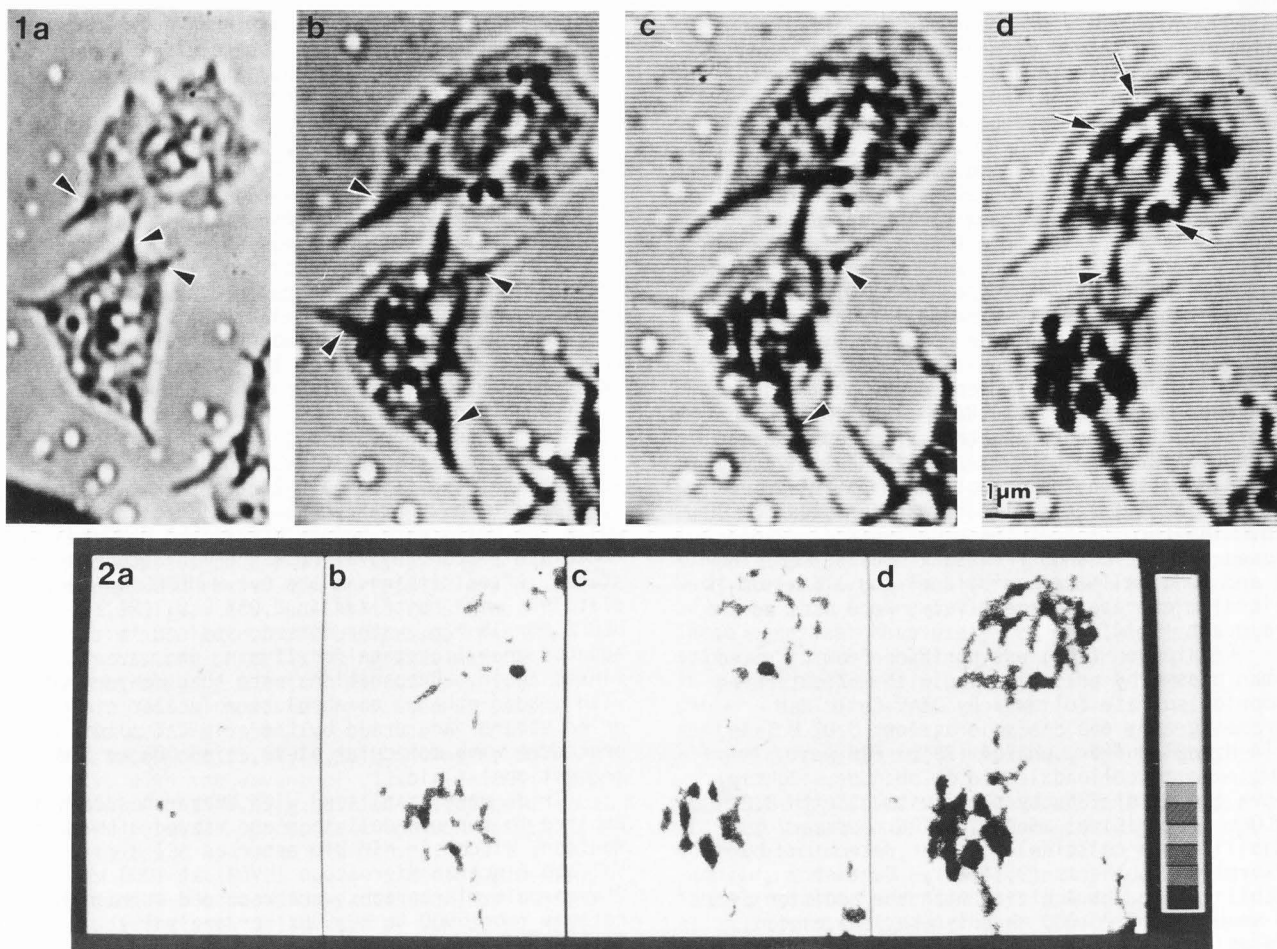


**Figure 1.** VLM of platelets adherent to PTMO-PEUU. Upper platelet in micrograph is at a more activated level of shape change than lower cell.  
 a) Platelets after 19 min of spreading are labeled with FGN-Au primarily on pseudopods (arrowheads). Upper platelet has ruffled, lightly labeled, edges.  
 b and c) At 24-30 min labeling of both platelets is heavier. FGN-Au has begun to move in towards the central granulomere. The edge of the upper cell is becoming less ruffled and is partially cleared of labels. Lower cell is labeled along pseudopods and along radial lines extending in from pseudopods over the hyaloplasm (arrowheads).  
 d) 36 min after adherence upper platelet is no longer spreading. FGN-Au is absent from cell periphery and is heavily concentrated in a circumferential ring around the granulomere. Lower platelet is still spreading. The most central densities may be due to granulomeric organelles. Note the densities in the pseudopod connecting the two cells (arrowhead). Arrows point out a few correlative label densities observed in Figures 2 and 3.

**Figure 2.** Digitized images of Figure 1a-d with the brighter half of the grey scale changed to white in order to emphasize dark, FGN-Au, labels. Threshold level was determined by comparison of recorded VLM image (at 36 min activation) to SEM and HVEM micrographs.

- a) Label is too diffuse thus the optical density is too low to show label at this threshold level.  
 b and c) Circumferential (upper platelet) and radial (lower platelet) densities are apparent.  
 d) Circumferential labeling is more apparent in upper platelet than earlier. Label has clearly moved centripetally and become more concentrated in both cells.

magnification of approximately 6000x. This magnification was chosen so that the diffracted image size of an individual 18 nm FGN-Au bead observed on glass (see Results and Discussion) was just larger than the width of an individual TV scan line.

The TV camera used was an instrumentation grade DAGE-MTI Newvicon (Michigan City, Indiana,

USA) modified for manual control of gain and black level. Further enhancement of contrast was achieved with a video processor (Colorado Video, 604 and 302-2, Boulder, Colorado, USA). Experiments were recorded with a high resolution video recorder (Panasonic NV9240XD, Secaucus, NJ, USA) for later playback and analysis. Micrographs were obtained by direct photography of the high

## Platelet Adhesion with Correlative Microscopies

resolution monitor (Panasonic WV-5410), or in some cases from the computer monitor with a 35mm camera fitted with a macro lens. Images were routed to the computer (IBM PC-XT fitted with Orchid and Tecmar video and graphic boards) for pseudocolor imaging and analysis of label location and density by grey-scale thresholding (see Results and Discussion).

### Results and Discussion

VLM and colloidal gold labeling was successfully employed to observe platelet spreading and FGN receptor motility of PEUU adherent human platelets. 18nm FGN-Au beads on polymer adherent platelets were not always individually visualized by VLM although individual 18nm FGN-Au particles were consistently visualized on glass. The visualization of FGN-Au binding to polymer adherent cells was achieved by the increased optical density of clustered labels on the platelet

surface. As label density increased the optical density increased from grey levels barely above background to the maximum black level of the video system. Thus label location was determined by darker areas on the cell surface while the relative darkness indicated label density (Figure 1). In many respects this is comparable to fluorescent microscopy in which several fluorochromes are necessary for detection. SEM and HVEM of identified cells, previously followed with VLM while living, demonstrates the good correlation of label location and density by all three methods of microscopy (Figures 1-3).

To facilitate imaging the optically dense FGN-Au labels, images were digitized and a grey scale threshold was applied. This process changed all pixels that were less dark than a user specified level to white, while pixels darker than the specified level were unaltered. Thus the position of the (darker) FGN-Au labels were emphasized by elimination of the background (Figure 2a-d). The interpretation of these thresholded micrographs must be performed with care since not all dark areas are due to label; edges and cell organelles can also produce dark regions (Figures 1-3). SEM or HVEM is necessary to absolutely determine label location although through-focus VLM is very helpful in this regard. For example, through-focus observation can determine if dark regions are on or in the cell. The threshold level is most easily determined by comparing the recorded VLM image with an electron micrograph of the same cell. The recorded VLM images may then be computed and observed during playback at the appropriate threshold level (Figure 2).

VLM observation of spreading platelets on all materials indicated that FGN-Au bound first to the cell periphery and along pseudopodia (Figures 1a-b and 2a-b). As the hyaloplasm extended, label density increased first at the cell periphery and then along radial spokes extending out over pseudopodia (Figures 1c-d and 2c-d). These radial densities gradually

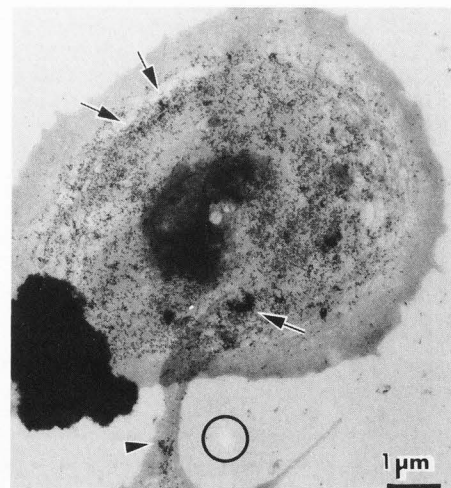
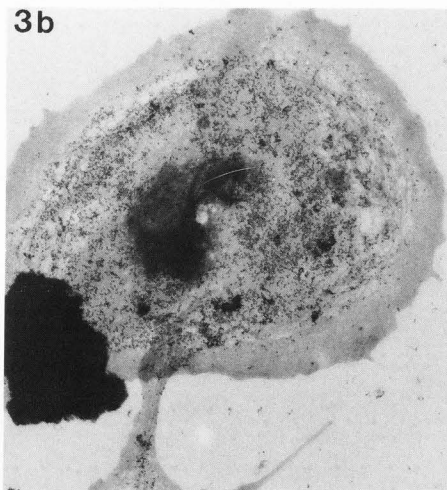
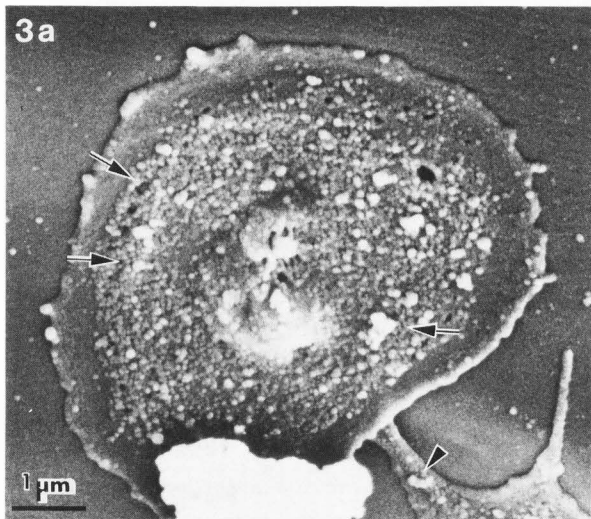


Figure 3. SEM (a) and HVEM stereo pair (b) of upper platelet in figures 1 and 2: Pseudopods extending into field are from lower cell. White object (SEM, dark in HVEM) is debris that attached during processing for electron microscopy. Note correlations of FGN-Au labels between these micrographs and figures 1d and 2d: Relative absence of label from cell periphery and over granulomere, localized densities of label on pseudopod (arrowhead) and at edge of FGN-Au labeled area (arrows). Note that the square impression on the underside of the film, due to replication of the NaCl crystal surface, is visualized with HVEM (b, circled) and not with SEM (a).

decreased as the label became centralized around the granulomere (Figures 1d and 2d). At all times label densities were observed to increase from the periphery to more centralized regions, although the possibility of individual receptors moving centrifugally or circumferentially cannot be ruled out by this observation. Platelets on other grids and different polymers fixed at various stages and observed by HVEM and SEM confirm label locations and the centripetal receptor motility as observed by VLM (Figures 4 and 5).

Differences in the extent of platelet spreading on these materials in the absence of exogenous FGN have been reported (7,8). The present study supports the previous observations that the shape change on Formvar is more extensive than on any of the PEUUs. Additionally, the observation that shape change was more extensive on the hydrophobic (large  $\gamma_{sw}$ , low  $\gamma_{sp}/\gamma_{sd}$ ) PDMS- and PTMO-PEUUs than on the more hydrophilic PPO- or PEO-PEUUs was also supported (7,8, and to be published). The level and pattern of FGN-Au binding and receptor motility for platelets on each of these polymers was consistent with the extent of each platelet's level of shape change, as reported by Loftus and Albrecht (24,25). Thus, more extensive labeling and label centralization were observed characteristically on the more activated platelets adherent to Formvar (Figure 5), followed by PTMO- or PDMS-PEUU adherent cells (Figures 1-3) than by those platelets on PPO- and PEO-PEUUs (Figure 4).

Preliminary studies were done to determine optimum label size for these investigations. Individual 12nm Au-FGN labels were more difficult to detect than 18nm labels by SEM, especially at magnifications appropriate for visualizing whole platelets. The 12nm labels also needed to be present in high density for reliable detection by VLM of polymer adherent platelets. Larger labels, of 24nm and 50nm diameter, were easily visible by SEM but localization of binding sites by HVEM was less precise, especially for the 50nm Au. VLM detectability of 24nm labels was not significantly better than for 18nm Au, possibly due to fewer labels binding per area as a consequence of steric hindrance. 50nm labels, while easily visible as individuals by VLM, bound in such low numbers that little information on receptor density could be obtained. Thus, 18nm Au was chosen as the best compromise for these studies. For studies of receptors present in lower numbers, or of receptors that do not co-migrate, larger labels might be required. Since the filmed grid perturbed cell visualization, VLM-SEM studies of such receptors on glass adherent cells could probably be done with 18nm or 24nm labels.

PEUU films were successfully prepared by a novel method of spin-casting. These polymers served as suitable support films for VLM and HVEM studies of adhesion to these (potential) bio-materials. VLM observation of platelets adherent to most of these materials was generally not as clear as that of platelets on Formvar, which in turn was significantly less clear than on glass.

Most of the reduction in image quality can be attributed to scatter at the film interfaces. The additional reduction of clarity seen with PEUU films was likely due to birefringence in the (circa 5nm size) microcrystalline domains present in these phase-segregated PEUU copolymers (11) which would affect polarization or DIC imaging. Video-enhanced asymmetric illumination contrast (V-AIC) microscopy was attempted to improve imaging since AIC is relatively unaffected by birefringent structures (18). However, we found visualization of platelets by V-AIC was less informative than with the V-DIC used in the present study. Video-enhanced brightfield and phase were also found less suitable for platelets adherent to filmed grids. An additional factor affecting the apparent quality of VLM images is the very shallow depth of field of DIC microscopy. When the microscope is focused on the cell surface, to best resolve labels, the cell edges are out of focus providing a less than esthetically pleasing image.

In contrast to the merely acceptable VLM properties of the PEUU films, these materials were excellent substrates for HVEM. The PEUU films met the major criteria for TEM supports including electron transparency, minimal intrinsic structure, and high mechanical stability under the electron beam (5). The PEUU filmed grids consistently exhibited greater stability in the HVEM than Formvar. Although holes and thickness variations were occasionally present as a consequence of replicating the NaCl crystal surface (Figure 3b), irradiation stability was sufficient to enable the recording of stereo-pair micrographs directly adjacent to these imperfections. Additionally, most of the PEUU films appeared visually homogeneous, with the notable exception of the PEO-PEUU. However, with stereo imaging this was of minimal consequence since the substrate can be clearly delineated from the cell by height or depth cues (Figure 4b). The stability of these films in the conventional TEM has yet to be determined.

In summary, correlative VLM, SEM and HVEM is useful in observing features of cell surface receptor expression and motility not possible to visualize by any one mode of microscopy. In particular, correlative light and electron microscopy allows living cells to be analyzed for their dynamic responses. Finally, the use of these novel support films permits in depth studies of the molecular biology of cell adhesion to a variety of synthetic surfaces with varied surface properties.

#### Acknowledgements

We wish to acknowledge the collaboration of Timothy G. Grasel and Stuart L. Cooper, Department of Chemical Engineering, University of Wisconsin. We thank Deane Mosher, Department of Medicine, University of Wisconsin, for the purified fibrinogen. This work was supported by grants from the NIH (HL-29596, HL-21001) and by a fellowship from the American Heart Association-Wisconsin Affiliate.

## Platelet Adhesion with Correlative Microscopies

### References

1. Albrecht RM, Oliver JA, Loftus JC. (1986). Observation of colloidal gold labelled platelet surface receptors and the underlying cytoskeleton using high voltage electron microscopy and scanning electron microscopy, in: *Science of Biological Specimen Preparation 1985*, M Muller, RP Becker, A Boyde, JJ Wolosewick (eds), SEM Inc., Chicago, IL, 185-193.
2. Allen RD, Allen NS, Travis JL. (1981). Video-enhanced contrast, differential interference contrast (AVEC-DIC) microscopy: a new method capable of analyzing microtubule-related motility in the reticulopodial network of *Allogromia laticollaris*. *Cell Motility* 1, 291-311.
3. Andrade JD, Ma SW, King, RN, Gregonis DE. (1972). Contact angles at the solid-water interface. *J. Coll. Interface. Sci.* 72, 488-494.
4. Baier RE, DePalma VA, Goupil DW, Cohen E. (1985). Human platelet spreading on substrata of known surface chemistry. *J. Biomed. Mater. Res.* 19, 1157-1167.
5. Baumeister W, Hahn M. (1978). Specimen

Supports, in: *Principles and Techniques of Electron Microscopy: Biological Applications*. Hayat MA (ed), Van Nostrand Reinhold, NY, 8, 1-112.

6. Goodman SL, Cooper SL, Albrecht RM. (1985). Activation of platelets from humans, canines and macaques on polymer surfaces. *Progress in Artif. Organs*, Y Nose, C Kjellstrand, P Ivanovich (eds), ISA Press, Cleveland, 1050-1055.
7. Goodman SL, Grasel TG, Cooper SL, Albrecht RM. (1986). Details of shape-change and fine structure of polyetherurethane - adherent human platelets. Abstracts, International Symposium on Artificial Organs, Biomedical Engineering and Transplantation. Salt Lake City, Utah, 3.
8. Goodman SL, Grasel TG, Cooper SL, Albrecht RM. (1986). Platelet shape-change and cytoskeletal reorganization on polyurethaneureas. *Society for Biomaterials Transactions*, 9, 46.

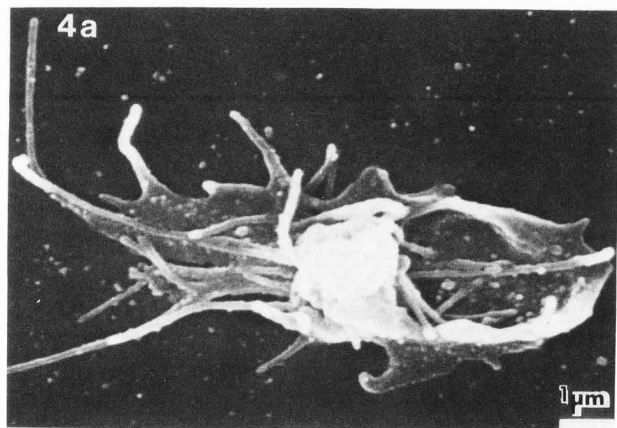


Figure 4. Platelets on PEO-PEUU:

- a) SEM micrograph showing pseudopodial morphology and relatively low level of shape change typical of platelets on this material. Note that label is relatively diffuse over the cell surface compared to labeling on more activated platelets.
- b) HVEM stereo pair of same cell as in figure 4a shows more clearly that most label is on pseudopods (arrowheads) or above microfilament bundles (arrows). Note variations in background density are in the PEO-PEUU support film.

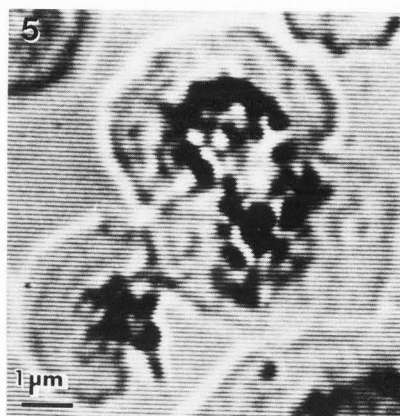
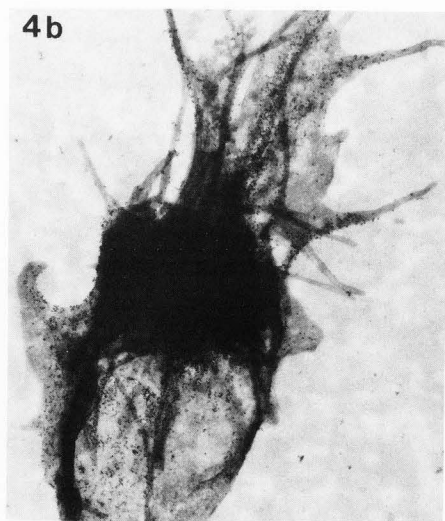


Figure 5. VLM of platelets adherent to Formvar 22 min after adherence. Note the extensive centralization and high density of FGN-Au label as compared to figures 1d and 2d.



9. Goodman SL, Hodges GM, Livingston DC. (1980). A review of the colloidal gold marker system. *Scanning Electron Microsc.* 1980; II:133-145.
10. Goodman SL, Lelah MD, Lambrecht LK, Cooper SL, Albrecht RM. (1984). In vitro vs. ex vivo platelet deposition on polymer surfaces. *Scanning Electron Microsc.* 1984; I:379-390.
11. Grasel TG, Cooper SL. (1986). Surface properties and blood compatibility of polyurethaneureas. *Biomaterials*, 7, 315-328.
12. Hall CE. (1966). *Introduction to Electron Microscopy*, McGraw-Hill, New York, 283-286.
13. Hamilton HC. (1972). A technique for the characterization of hydrophilic solid surfaces. *J. Colloid. Interfac. Sci.*, 10, 219-222.
14. Horisberger W, Rosset J, Baurer H. (1975). Colloidal gold granules as markers for cell surface receptors in the scanning electron microscope. *Experientia*, 31, 1147-1149.
15. Inoue S. (1981). Video image processing greatly enhances contrast, quality, and speed in polarization-based microscopy. *J. Cell Biol.*, 89, 346-356.
16. Inoue S, Hyde WL. (1957). Studies on depolarization of light at microscope lens surfaces: II. The simultaneous realization of high resolution and high sensitivity with the polarizing microscope. *J. Biophysic. Biochem. Cytol.*, 3(6), 831-843.
17. Jaycock MJ, Parfitt JD. (1981). *Chemistry of Interfaces*, Ellis Harwood Ltd., West Sussex, England, 240.
18. Kachar B. (1985). Asymmetric Illumination Contrast: A Method of Image Formation for Video Light Microscopy. *Science*, 227, 766-768.
19. Lelah MD, Jordan CA, Pariso ME, Lambrecht LK, Cooper SL, Albrecht RM. (1983). The morphology of platelet and thrombus deposition on biomaterials in a canine ex-vivo series shunt. *Scanning Electron Microsc.* 1983; IV: 1983-1994.
20. Lelah MD, Lambrecht LK, Young BR, Cooper SL. (1983). Physicochemical characterization and in vivo blood tolerability of cast and extruded Biomer. *J. Biomed. Mater. Res.*, 17, 1-22.
21. Lelah MD, Pierce JA, Cooper SL. (1985). The measurement of contact angles on circular tubing surfaces using the captive bubble technique. *J. Biomed. Mater. Res.*, 19, 1011-1015.
22. Lewis JC, Prater T, Taylor RG, White MS. (1980). The use of correlative SEM and TEM to study thrombocyte and platelet adhesion to artificial surfaces. *Scanning Electron Microsc.* 1980; III:189-202.
23. Lewis JC, White MS, Prater T, Porter KR, Steele RJ. (1985). Three-dimensional organization of the platelet cytoskeleton during adhesion in vitro: Observations on human and nonhuman cells. *Cell Motility*, 3, 589-608.
24. Loftus JC, Albrecht RM. (1983). Use of colloidal gold to examine fibrinogen binding to human platelets. *Scanning Electron Microsc.* 1983; IV:1995-1999.
25. Loftus JC, Albrecht RM. (1984). Redistribution of the fibrinogen receptor of human platelets following surface activation. *J. Cell Biol.*, 99, 822-829.
26. Loftus JC, Choate J, Albrecht RM. (1984). Platelet activation and cytoskeletal reorganization: HVEM examination of intact and Triton extracted whole mounts. *J. Cell Biol.*, 98, 2019-2025.
27. Maupin-Szamier P, Pollard TD. (1978). Actin filament destruction by osmium tetroxide. *J. Cell Biol.*, 77, 837-852.
28. Mosher DF. (1975). Cross-linking of cold insoluble globulin by fibrin stabilizing factor. *J. Biol. Chem.*, 250, 6614-6621.
29. Okano T, Kataoka K, Sakurai Y, Shimada M, Miyahara M, Akaïke T, Shinohara I. (1981). Molecular design of block and graft copolymers having the ability to suppress platelet adhesion. *Artif. Organs*, 5(suppl.), 468-470.
30. Oliver JA, Albrecht RM. (1987). Colloidal gold labelling of fibrinogen receptors in epinephrine- and ADP- activated platelet suspensions. *Scanning Microsc.*, 1(2), 745-756.
31. Peerschke EIB. (1985). The platelet fibrinogen receptor. *Seminars in Hematology*, 22, 241-259.
32. Ratner BD. (1985). Graft copolymer and block copolymer surfaces. in: *Surface and Interfacial Aspects of Biomedical Polymers*. JD Andrade (ed), Plenum Press, NY, 373-394.
33. Zucker MB, Peerschke EI. (1980). Specific binding of fibrinogen to platelets: Relationship to shape change and aggregation. in: *Platelets: Cellular Response Mechanisms and their Biological Significance*. A Rotman, FA Meyer, C Gitler, A Silberberg (eds), John Wiley and Sons Ltd., NY, 157-168.

#### Discussion with Reviewers

**M. D. Lelah:** Was any attempt made to examine the roughness and texture of both the NaCl crystal cut face and the urethane coated surface? A smoother cut face may result in a smoother urethane film surface, and thus a better quality image, for these very thin films.

**Authors:** We made no systematic examination although we consistently observed that the film appeared to accurately replicate the NaCl crystal surface hence film surfaces should have been smooth to molecular dimensions. Microscopic observation appeared to confirm this. Often the uniformity of the polyurethane film was affected by crystal surface roughness as a consequence of the replication of crystal imperfections (slip planes and other dislocations). However, this did not generally affect observation since the films were usually uniform over several hundred square microns.

**Reviewer III:** Please comment on the reasons why we do not see identical features on Figs. 3b (stereo-pair) and Figs. 1d and 2d? How do you know the dark circles on Fig. 3b are not dense granules?

**Authors:** Correspondence between VLM and EM images are less than exact due to the difference in the physics of image formation for the different microscopic modes. The resolution and depth of fields are different in various microscopy methods. In addition, Fig. 1d is of living platelets while the micrographs in Figs. 3a and 3b are of one of these cells after fixation. It is possible that small changes in cell shape occur as the initial fixative reacts, hence this could account for some inexactness in the correlation between images.